Cold Collision Frequency Shifts in a ^{87}Rb Atomic Fountain

Y. Sortais, S. Bize, C. Nicolas, and A. Clairon
BNM-LPTF, Observatoire de Paris, 61 avenue de l'Observatoire, 75014 Paris, France

C. Salomon
Laboratoire Kastler Brossel, ENS, 24 rue Lhomond, 75005 Paris, France

C. Williams
National Institute of Standards and Technology, 100 Bureau Drive, Gaithersburg, Maryland 20899-8423
(Received 26 May 2000)

We present measurements of cavity frequency pulling and collisional frequency shifts in a ^{87}Rb fountain with a frequency resolution of 3×10^{-16}. Agreement with theory is found for the cavity pulling and the measured collisional shifts. The clock shift is found at least 50 times smaller than in ^{133}Cs.

PACS numbers: 32.80.Pj, 06.30.Ft, 34.20.Cf

In the last 10 years, our understanding of the physics of collisions between ultracold atoms has improved considerably [1]. Data from photoassociation spectroscopy [2], frequency shifts in atomic clocks [3,4], Bose-Einstein condensation [5,6], and Feshbach resonances [7] are now strongly constraining the interatomic potentials. Collisions play a crucial role in high precision clocks using laser cooled atoms. The current accuracy of Cs clocks, on which the SI second is based, now reaches 1.1×10^{-15}, using a fountain geometry [8]. Since interactions between cold atoms represent a major part in the inaccuracy budget, Cs fountains operate at low atomic density, hence with a small number of atoms, typically less than 10^6. Even with detection at the fundamental quantum projection noise, this sets a limit to the frequency stability [9]. In 1997, Kokkelmans *et al.* predicted that the collisional frequency shift for ^{87}Rb was 15 times smaller than for ^{133}Cs [10]. Rubidium fountains could then operate with larger atom numbers and represent an attractive alternative to Cs frequency standards. In this Letter, we show that another effect which depends linearly on the atom number must be considered, namely the cavity pulling frequency shift, well known in hydrogen masers [11]. Our treatment of the frequency shift measurements takes into account both collisional shift and cavity pulling simultaneously. By tuning the cavity around the Rb resonance frequency, we display the characteristic dispersive line shape of the cavity pulling effect and find good agreement with theory with a relative frequency resolution of 3×10^{-16}. A quantitative model of the pulling effect allows us to make a precise determination of the number of atoms crossing the cavity. After subtraction of its contribution, we measure collisional frequency shifts in marginal agreement with the predictions of Ref. [10] and reasonable agreement with the more recent predictions of [12].

In a fountain standard, the atoms interact twice with a microwave field (Ramsey method), inducing transitions between two internal states $|\alpha\rangle$ and $|\beta\rangle$. The collisional frequency shift is due to the interaction between atoms inside the atomic cloud during the interrogation period. At very low temperatures, only s-wave scattering occurs and the collision physics is described using a single parameter, the scattering length a. For a nondegenerate gas of N atoms in state α, the total mean-field energy shift is equal to $(4\pi\hbar^2/m)a\bar{n}_\alpha N$, where $\bar{n}_\alpha$ is the average atomic density in state $|\alpha\rangle$. In the fountain, when all the population is transferred from $|\alpha\rangle$ to $|\beta\rangle$, the collisional frequency shift is given by $2\pi\Delta\nu = (4\pi\hbar/m)(a_{\beta\beta} - a_{\alpha\alpha})\bar{n}$, where $a_{\alpha\alpha}$ ($a_{\beta\beta}$) is the scattering length for two atoms colliding in the internal state $|\alpha\rangle$ ($|\beta\rangle$). We will also consider more general cases where states other than α and β are populated. The mean-field shift is then given by [10]

$$\Delta\nu = -\frac{2\hbar}{m} \times \sum_j n_j(1 + \delta_{\alpha,j})(1 + \delta_{\beta,j})(a_{\alpha,j} - a_{\beta,j}). \tag{1}$$

The j index refers to the atomic Zeeman substate $|F, m_F\rangle$. $\alpha = |1, 0\rangle$ and $\beta = |2, 0\rangle$ are the lower and higher clock levels. The Kronecker symbol δ_{ij} accounts for quantum statistics. In a fountain, the partial densities n_j are space and time dependent, and the measured frequency shifts appear as an average over these variables.

The second effect which depends on atom number is the cavity frequency pulling [11]. In our fountain, the atomic transition is probed by a 6.8 GHz microwave field in a TE_{011} copper resonator with a quality factor $Q \simeq 10^4$. The pulling effect is due to the interference inside the microwave resonator between the field radiated by the input coupler and the field radiated by the atomic magnetic dipoles when the atoms pass through the cavity. This interference induces a time dependent phase shift between the field inside the resonator and the signal delivered by the oscillator. It produces a clock shift that exhibits a dispersive dependence as a function of the cavity detuning with respect to the atomic resonance ($\Delta\nu_{\text{cav}} = \nu_{\text{cav}} - \nu_{\text{at}}$). The width of this dispersion curve is proportional to $1/Q$. The amplitude is proportional both to Q and to the number of atoms crossing the cavity. When the atoms enter the

cavity in the upper state (lower state) and deposit (extract) energy in the cavity, the clock frequency is *pulled* towards (*pushed* away from) the cavity resonance frequency.

Our laser cooled ^{87}Rb fountain has been described in a previous paper [13]. First, in 1 s, up to 7×10^8 atoms are captured in a magneto-optical trap (MOT) with 6 laser beams of power 20 mW, diameter 3 cm, and tuned to the $F = 2 \rightarrow F' = 3$ transition at 780 nm. A 200 ms molasses phase at $\delta = -5\Gamma$ ($\Gamma = 2\pi \times 6$ MHz) allows for the MOT magnetic field decay. The atoms are then launched upwards at $\sim 3.5\ \mathrm{m\,s^{-1}}$ in 2 ms and cooled down to an effective temperature of $\sim 1.2\ \mu$K. After launch, atoms can be selected in a specific Zeeman substate by means of microwave and laser pulses. Atoms interact twice with a 6.8 GHz microwave field synthesized from a high stability quartz oscillator weakly locked to the output signal of an H maser. The two $\pi/2$ Ramsey interactions are separated by $\sim$400 ms. The number of atoms $N_{F=1}$ ($N_{F=2}$) in both hyperfine levels are then measured by time of flight fluorescence (TOF) induced by a pair of laser beams located below the MOT. From the transition probabilities $N_{F=2}/(N_{F=1} + N_{F=2})$ measured on both sides of the central Ramsey fringe, we compute an error signal to lock the microwave interrogation frequency to the atomic transition using a digital servo loop.

Our measurement approach uses a differential method. Every 200 fountain cycles ($\sim$350 s), we change the trapping light intensity so that the number of atoms in the fountain alternates between two values N_{high} and $N_{\mathrm{low}} \simeq N_{\mathrm{high}}/4$. We measure the frequency difference between the two situations. This method efficiently rejects slow frequency fluctuations which are not related to atom number or density, in particular the H-maser drift. In the differential method the frequency resolution is $\sim 3 \times 10^{-13}\tau^{-1/2}$ where τ is the averaging time in seconds. At 350 s the maser stability is $\sim 2.7 \times 10^{-15}$, at least 4 times better than the fountain stability. The relative frequency resolution on effects which depend on atom number reaches $\sim 1 \times 10^{-15}$ per day.

After launch, atoms are spread among the various m_F substates of the $F = 2$ manifold. Data have been taken in three cases. (i) Normal clock operation: atoms in the $|2, 0\rangle$ substate are transferred to $|1, 0\rangle$ using a microwave π pulse. Atoms remaining in $|2, m_F \neq 0\rangle$ are pushed away by radiation pressure. Only three scattering lengths $a_{\alpha\alpha}$, $a_{\alpha\beta}$, and $a_{\beta\beta}$ in Eq. (1) are involved. (ii) No selection: all Zeeman sublevels in $F = 2$ are equally populated to within 2%–3%. The frequency shift of the $|2, 0\rangle \rightarrow |1, 0\rangle$ transition is measured in the presence of $|2, m_F \neq 0\rangle$ populations. (iii) Atoms are pumped in $F = 1$ by a laser pulse tuned to the $F = 2 \rightarrow F' = 2$ optical transition. Atoms remaining in the $F = 2$ state ($\leq$2%) are pushed away by radiation pressure. The launched atoms are equally spread among the $F = 1$ substates to within 1%. The frequency shift of the $|1, 0\rangle \rightarrow |2, 0\rangle$ transition is measured in the presence of $|1, m_F \neq 0\rangle$ populations.

In order to compare the frequency measurements with cavity pulling and collisional shift predictions, great care has been taken to measure precisely both the number of atoms entering the microwave resonator and the average atomic density during the Ramsey interrogation. The initial atom number is determined by two methods: first, an absorption method performed at the end of the cooling process with an uncertainty of $\sim$20%; second, a detailed analysis of the TOF signals and detection efficiency, which requires a precise knowledge of the initial spatial and velocity distributions. The spatial distribution is obtained by imaging the fluorescence of the cloud onto a CCD camera in the molasses phase 500 μs before launch, and by measuring the absorption signal for various apertures of the probe beam. We find a Gaussian distribution with $\sigma = 1.4$ mm for $N_{\mathrm{high}} = 4 \times 10^8$ atoms, and $\sigma = 0.85$ mm for $N_{\mathrm{low}} = 8 \times 10^7$ atoms. The velocity distribution is deduced from the time of flight signals in the detection zone. They clearly exhibit a non-Gaussian shape (Fig. 1a) that we model by a 3D isotropic distribution $(1 + |\vec{v} - \vec{v}_l|^2/v_0^2)^{-b}$ law, v_0 and b being the free parameters of the fit. This analytical distribution is theoretically predicted by [14] and exhibits large wings as expected near the threshold of operation of the optical molasses. Operating in this regime is necessary in our experiment in order to obtain the lowest temperature and thus the highest atomic densities. In cases (i) and (ii), we find $v_0 \sim 18\ \mathrm{mm\,s^{-1}}$, whereas $v_0 \sim 23\ \mathrm{mm\,s^{-1}}$ in case (iii) because of optical pumping. In all three cases, we find $b \sim 2$. These values are monitored during data acquisition. A numerical simulation provides the time dependent atomic density and number in the fountain. The calculated fraction of atoms passing in the detection zone is compared with the TOF measurements for various launch velocities in Fig. 1b. This constitutes a test of the 3D velocity distribution. We also deduce the number of atoms entering the microwave cavity and in the detection zone, and good agreement is found (20%) with the calibrated detection.

Partial densities n_j in Eq. (1) are time dependent for two reasons. First, the atomic cloud expands during the Ramsey interrogation: the peak atomic density typically varies by a factor of $\sim$30 during the Ramsey interrogation. Second, the atomic populations of the $|1, 0\rangle$ and $|2, 0\rangle$ levels change during the two microwave interactions. We take into account in our simulation the nonuniform sensitivity of the clock frequency to a time dependent perturbation of the atomic frequency [15]. We calculate the time averaged partial densities $\langle n_j \rangle_t$ that each detected atom encounters during its ballistic flight. Then, we average over the initial spatial and velocity distributions to determine the *effective* partial densities $\bar{n}_j = \langle n_j \rangle_{t,\vec{r},\vec{v}}$, used in Eq. (1) for comparison with theory. The total effective atomic density is

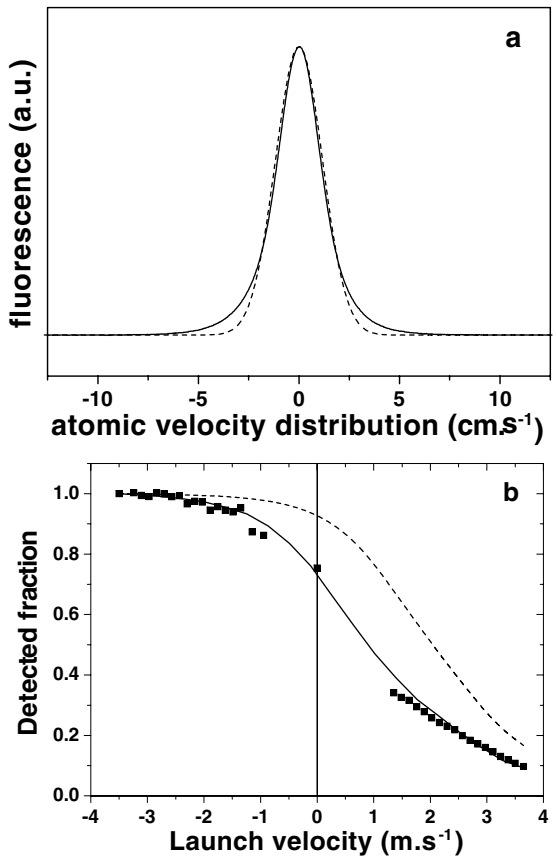

FIG. 1. (a) Velocity distribution of the atoms in the moving frame. The fit with a square of a Lorentzian (see text) cannot be distinguished from the data (solid line). The Gaussian fit (dotted line) is clearly not adequate. (b) Fraction of detected atoms as a function of the launch velocity (squares). Solid line: numerical simulation. Dotted line: Gaussian velocity distribution.

$\bar{n} = \sum_j \bar{n}_j$. Typically, in case (i) with $N_{\text{high}} = 4.3 \times 10^7$, $\bar{n} = 1.5 \times 10^7$ cm^3.

Figure 2 shows the differential measurement of the clock frequency shift as a function of the cavity detuning

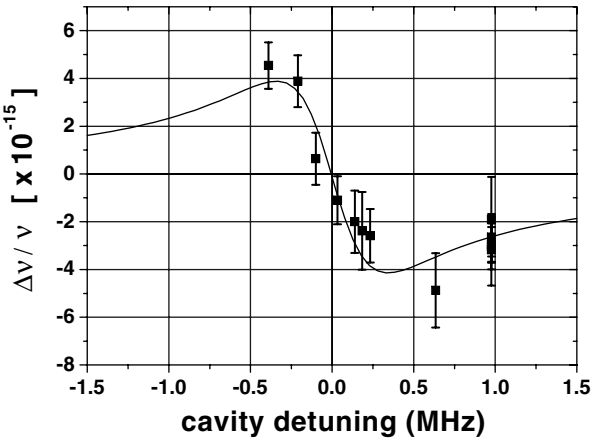

FIG. 2. Relative frequency shift vs cavity detuning for $\Delta N = 3.5 \times 10^7$ in case (i). Solid line: fit from Eq. (2).

$\Delta\nu_{\text{cav}}$ with respect to the atomic resonance, for atoms initially selected in $|1,0\rangle$, with $N_{\text{high}} \simeq 4.3 \times 10^7$ entering the microwave cavity and $N_{\text{low}} \simeq 0.8 \times 10^7$. The simulation shows that this modulates the effective density by a factor of $\sim$3.3. The frequency and quality factor of the cavity are measured with an uncertainty of 20 kHz and 4%, respectively, and the cavity is tuned by temperature [16]. The solid line is a least squares fit of the data using the following function:

$$\delta\nu/\nu = A[f(\Delta\nu_{\text{cav}})\Delta N + B\Delta\bar{n}], \qquad (2)$$

where A and B are the free parameters of the fit, and $\Delta N = N_{\text{high}} - N_{\text{low}}$ [17]. $f(\Delta\nu_{\text{cav}})$ is the calculated dispersive line shape of the cavity pulling effect for a single atom in the cavity. A is a common scale factor on the atom number and is expected to be 1. We find $A = 1.26(14)$ and $B = -7.2(20.0) \times 10^{-24}$ cm^3. Thus, the number of atoms determined by the cavity pulling effect has an uncertainty of 11% and agrees with the measurements described above, within the combined error bars. This more precise determination of N is now used for the evaluation of the collisional shift. B, the collisional shift coefficient, is surprisingly consistent with zero even with a frequency standard deviation of 3×10^{-16} given by the fit. Thus in case (i), at a density of 1.5×10^7, ^{87}Rb exhibits no detectable shift [Fig. 3(i)], whereas ^{133}Cs would exhibit a shift of 3×10^{-14}.

Figure 3 summarizes the collisional shifts measurements versus the effective density $\bar{n}$ [18]. By contrast to case (i), data recorded in cases (ii) and (iii) show a clear dependence with the density after subtracting the cavity pulling effect. The measured value in case (ii) $-50(10)\,(^{+22}_{-34}) \times 10^{-24}$ cm^3 is in reasonable agreement with -56×10^{-24} cm^3 (Ref. [10]) and -33×10^{-24} cm^3 (Ref. [12]). The first set of parentheses refers to the frequency statistical uncertainty (1 standard deviation); the second set refers to the linear combination of frequency uncertainty and density calibration uncertainty. From variations of the parameters in the simulation and experimental calibrations, we deduce a 35% type B uncertainty on our density. Adding quadratically the 11% statistical uncertainty on atom number, we get a 40% combined uncertainty on the density. This corresponds to a scale factor of 1.4 and $1/1.4$ on the density axis of Fig. 3, defining the acceptance domain of the measurements (dotted lines). In case (iii), the agreement is similar. We find $-60(16)\,(^{+29}_{-46}) \times 10^{-24}$ cm^3 to be compared to -68×10^{-24} cm^3 (Ref. [10]) and -41×10^{-24} cm^3 (Ref. [12]). Finally, our data in case (i), $-7.2(20.0)\,(^{+25}_{-31}) \times 10^{-24}$, show a disagreement at $\sim 3\sigma$ with the theory of Ref. [10] and seem to favor the more recent theory of Ref. [12].

In summary, the smallness of the ^{87}Rb clock transition collisional shift makes this atom very attractive for high accuracy microwave frequency standards. When

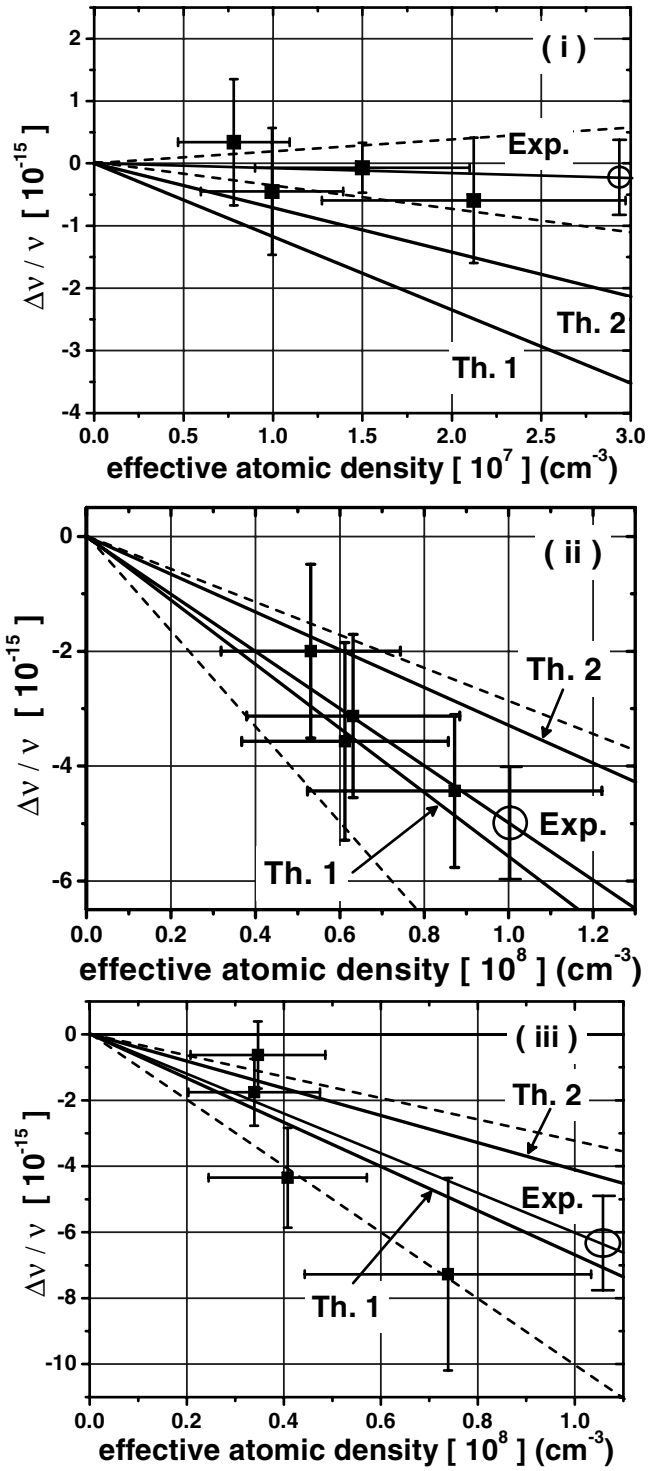

FIG. 3. Relative frequency shift of the $|1,0\rangle \rightarrow |2,0\rangle$ transition vs effective density in cases (i), (ii), and (iii) (atoms initially selected in states $|1,0\rangle$, $|2,m_F = 0,\pm 1,\pm 2\rangle$ equally populated and $|1,m_F = 0,\pm 1\rangle$ equally populated, respectively), and comparison with theories of Ref. [10] (Th.1) and Ref. [12] (Th.2). Open circles: linear fits to the experimental data with corresponding statistical frequency uncertainty at the given density. Horizontal error bars represent the 40% density uncertainty. Dotted lines: experiment with combined frequency and density uncertainties.

detecting $\sim 2 \times 10^7$ atoms and with a suitable interrogation oscillator, the quantum limited stability should reach $\sim 1 \times 10^{-14}\tau^{-1/2}$ down to 3×10^{-17} at one day.

We acknowledge fruitful discussions with Y. Castin, C. Cohen-Tannoudji, J. Dalibard, G. Shlyapnikov, P. Laurent, P. Lemonde, G. Santarelli, C. Mandache, and the ENS cold atom group. This work was supported in part by BNM and CNRS. BNM-LPTF and Laboratoire Kastler Brossel are Unités Associées au CNRS, UMR 8630, and UMR 8552.

Note added.—After completing this work we learned that related work was performed by C. Fertig and K. Gibble where a nonzero shift in case (i) was measured [19]. Their value of $-0.38(8)$ mHz at $1.0(6) \times 10^9$ cm^{-3} is consistent with our measurements.

[1] *Bose-Einstein Condensation in Atomic Gases,* Proceedings of the International School of Physics "Enrico Fermi," Course 140 (IOS Press, Washington, DC, 1999).
[2] H. M. J. M. Boesten, C. C. Tsai, B. J. Verhaar, and D. J. Heinzen, Phys. Rev. Lett. **77**, 5194 (1996).
[3] K. Gibble and S. Chu, Phys. Rev. Lett. **70**, 1771 (1993).
[4] S. Ghezali, P. Laurent, S. N. Lea, and A. Clairon, Europhys. Lett. **36**, 25 (1996).
[5] D. Stamper-Kurn *et al.,* Phys. Rev. Lett. **81**, 2194 (1998).
[6] M. R. Matthews *et al.,* Phys. Rev. Lett. **81**, 243 (1998).
[7] V. Vuletić, A. Kerman, C. Chin, and S. Chu, Phys. Rev. Lett. **82**, 1406 (1999).
[8] P. Laurent *et al.,* in Proceedings of the International Conference on Laser Spectroscopy (World Scientific, London, 1999), p. 41.
[9] G. Santarelli *et al.,* Phys. Rev. Lett. **82**, 4619 (1999).
[10] S. J. J. M. F. Kokkelmans, B. Verhaar, K. Gibble, and D. Heinzen, Phys. Rev. A **56**, R4389 (1997).
[11] J. Vanier and C. Audoin, *The Quantum Physics of Atomic Frequency Standards* (Adam Hilger, Philadelphia, 1989).
[12] C. Williams *et al.* (private communication).
[13] S. Bize *et al.,* Europhys. Lett. **45**, 558 (1999).
[14] Y. Castin, J. Dalibard, and C. Cohen-Tannoudji, *Light Induced Kinetic Effects on Atoms, Ions and Molecules* (ETS Editrice, Pisa, 1991), p. 5.
[15] P. Lemonde *et al.,* in *Proceedings of Frequency Control Symposium* (IEEE, Piscataway, NJ, 1998) p. 110.
[16] C. Fertig and K. Gibble, IEEE. Trans. Instrum. Meas. **48**, 520 (1999).
[17] In Fig. 2 we have rescaled the data to a fixed $\Delta N = 3.5 \times 10^7$. During the 6 month data acquisition, ΔN typically fluctuated by 20%, v_0 by 7%, and b by 6%.
[18] To clarify Fig. 3(i), we represent, in place of individual measurements, the weighted average of 10 of them performed at very similar densities [$1.5(2) \times 10^7$ cm^{-3}].
[19] C. Fertig and K. Gibble, Phys. Rev. Lett. **85**, 1622 (2000).